

NAXE Mutations Disrupt the Cellular NAD(P)HX Repair System and Cause a Lethal Neurometabolic Disorder of Early Childhood

Laura S. Kremer,^{1,2,16} Katharina Danhauser,^{3,16} Diran Herebian,^{3,16} Danijela Petkovic Ramadža,⁴ Dorota Piekutowska-Abramczuk,⁵ Annette Seibt,³ Wolfgang Müller-Felber,⁶ Tobias B. Haack,^{1,2} Rafał Płoski,⁷ Klaus Lohmeier,³ Dominik Schneider,⁸ Dirk Klee,⁹ Dariusz Rokicki,¹⁰ Ertan Mayatepek,³ Tim M. Strom,^{1,2} Thomas Meitinger,^{1,2,11} Thomas Klopstock,^{11,12,13} Ewa Pronicka,^{5,10} Johannes A. Mayr,¹⁴ Ivo Baric,^{4,15} Felix Distelmaier,^{3,16,*} and Holger Prokisch^{1,2,16,*}

To safeguard the cell from the accumulation of potentially harmful metabolic intermediates, specific repair mechanisms have evolved. *APOA1BP*, now renamed *NAXE*, encodes an epimerase essential in the cellular metabolite repair for NADHX and NADPHX. The enzyme catalyzes the epimerization of NAD(P)HX, thereby avoiding the accumulation of toxic metabolites. The clinical importance of the NAD(P)HX repair system has been unknown. Exome sequencing revealed pathogenic biallelic mutations in *NAXE* in children from four families with (sub-) acute-onset ataxia, cerebellar edema, spinal myelopathy, and skin lesions. Lactate was elevated in cerebrospinal fluid of all affected individuals. Disease onset was during the second year of life and clinical signs as well as episodes of deterioration were triggered by febrile infections. Disease course was rapidly progressive, leading to coma, global brain atrophy, and finally to death in all affected individuals. *NAXE* levels were undetectable in fibroblasts from affected individuals of two families. In these fibroblasts we measured highly elevated concentrations of the toxic metabolite cyclic-NADHX, confirming a deficiency of the mitochondrial NAD(P)HX repair system. Finally, NAD or nicotinic acid (vitamin B3) supplementation might have therapeutic implications for this fatal disorder.

Whereas chemical modification or degradation and repair of macromolecules such as DNA and proteins are well-recognized processes, damage and repair of metabolites only recently has become an emerging field of research. Aberrant metabolites can arise either spontaneously or by enzymatic side reactions and can result in neutral or harmful species. To prevent toxic effects on the cell, damage-control systems have developed that either remove or recycle the aberrant metabolite.¹ Nicotinamide adenine dinucleotide (reduced form, NADH; oxidized form, NAD⁺) and nicotinamide adenine dinucleotide phosphate (reduced form, NADPH; oxidized form, NADP⁺) are major redox equivalents in the cell involved in either catabolic or anabolic reactions as well as reactions involved in protection against reactive oxygen species (ROS). One of the double bonds of the nicotinamide ring present in NADH and NADPH is prone to hydration. This hydration can occur either spontaneously at mildly acidic pH or at elevated temperature (already relevant at 37°C) or enzymatically, e.g., as a side reaction of the glyceraldehyde 3-phosphate dehydrogenase (GAPDH). NAD(P)HX is

formed as R- and S-epimers.^{2,3} Neither NADHX nor NADPHX can act as electron donors or acceptors and have been shown to inhibit several dehydrogenases, making the aberrant metabolites not only dispensable but toxic. NAD(P)HX can further spontaneously react to cyclic-NAD(P)HX in an irreversible way (for schematic overview see Figure 1). Whereas no repair system is known for the cyclic form of NAD(P)HX, reconversion of NAD(P)HX to NAD(P)H is catalyzed by an ATP-dependent dehydratase.⁴ This dehydratase, now renamed NAXD (previously CARKD [MIM: 615910]), reacts only with the S-epimer of NAD(P)HX. In order to eliminate the R-epimer, a specific epimerase, which is encoded by *NAXE* in humans (MIM: 608862), catalyzes the conversion to S-NADHX. Deficiency of the epimerase in *S. cerevisiae* strains did not affect viability and growth.^{4,5} Even in the multicellular organism *A. thaliana*, knockdown of the dehydratase resulted in no observable phenotype.⁶ Therefore, the physiological importance of this repair system remains unclear in these species. Effects of an enzyme deficiency in humans have not been analyzed so far.

¹Institute of Human Genetics, Technische Universität München, 81675 München, Germany; ²Institute of Human Genetics, Helmholtz Zentrum München, 85764 Neuherberg, Germany; ³Department of General Pediatrics, Neonatology and Pediatric Cardiology, University Children's Hospital, Heinrich-Heine-University Düsseldorf, 40225 Düsseldorf, Germany; ⁴Department of Pediatrics, University Hospital Center, 10000 Zagreb, Croatia; ⁵Department of Medical Genetics, The Children's Memorial Health Institute, 04-730 Warsaw, Poland; ⁶Department of Pediatric Neurology and Developmental Medicine, Ludwig-Maximilians-University, 80337 Munich, Germany; ⁷Department of Medical Genetics, Warsaw Medical University, 02-106 Warsaw, Poland; ⁸Clinic of Pediatrics, 44137 Dortmund, Germany; ⁹Department of Diagnostic and Interventional Radiology, University Düsseldorf, Medical Faculty, 40225 Düsseldorf, Germany; ¹⁰Department of Pediatrics, Nutrition and Metabolic Diseases, Department of Medical Genetics, The Children's Memorial Health Institute, 04-730 Warsaw, Poland; ¹¹Munich Cluster for Systems Neurology (SyNergy), 81377 Munich, Germany; ¹²Department of Neurology, Friedrich-Baur-Institute, Ludwig-Maximilians-University, 80336 Munich, Germany; ¹³German Center for Neurodegenerative Diseases (DZNE), 80336 Munich, Germany; ¹⁴Department of Pediatrics, Paracelsus Medical University, 5020 Salzburg, Austria; ¹⁵School of Medicine, University of Zagreb, 10000 Zagreb, Croatia

¹⁶These authors contributed equally to this work

*Correspondence: felix.distelmaier@med.uni-duesseldorf.de (F.D.), prokisch@helmholtz-muenchen.de (H.P.)
<http://dx.doi.org/10.1016/j.ajhg.2016.07.018>

© 2016 American Society of Human Genetics.

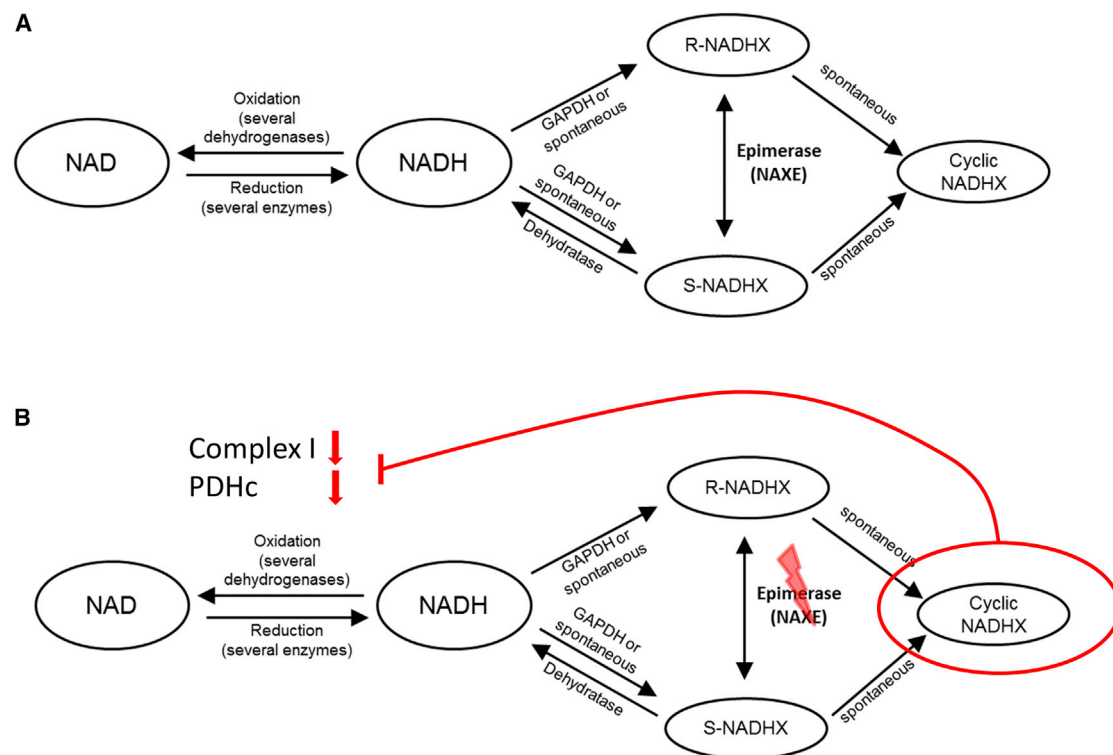


Figure 1. Schematic Overview of NAD/NADH Metabolism and the NAD(P)HX Repair System

(A) NAD(P)HX repair system at metabolic equilibrium under normal/healthy conditions.

(B) Putative consequences of NAXE deficiency, leading to increased formation of cyclic NADHX, a toxic inhibitor of cellular NADH dehydrogenases.

In this study, we report on a joint investigation of whole-exome sequencing (WES) datasets of a cohort of 600 individuals recruited within the German and European network for mitochondrial disorders (mitoNET and GENOMIT) to elucidate the molecular basis of the disease using a previously described bioinformatic filtering pipeline^{7,8} that identified three affected individuals carrying rare biallelic variants in *NAXE*. A fourth family with *NAXE* mutations was discovered by WES independently. The predominant clinical features found in these subjects include (sub-) acute onset of ataxia, cerebellar edema, spinal myelopathy, and skin lesions (summarized in Table 1). Neuroimaging findings and skin manifestations are depicted in Figure 2 and detailed case reports as well as additional neuroimaging findings are provided in the Supplemental Data. Written informed consent was obtained from the guardians of all individuals investigated. The study was approved by the local ethics committees.

Exome sequencing of affected individuals from families F1, F2, and F3 was performed in Germany using the SureSelect Human All Exon 50 Mb kit (Agilent) for in-solution enrichment of exonic regions followed by sequencing as 100 base pair (bp) paired-end runs on a HiSeq2500 (Illumina).^{7,8} Read alignment to the human genome (UCSC Genome Browser build hg19) was done with Burrows-Wheeler Aligner (BWA, v.0.7.5a)⁹ and single-nucleotide variants and small insertions and deletions were detected with BWA (v.0.7.5a) and SAMtools (version 0.1.19). We

achieved an average fold coverage between 134 and 148 with 97.5% of the exome covered at least 20-fold. Sequencing analysis of individuals #1-1, #2, and #3 did not identify mutations in disease-associated genes that would account for the phenotype. Per individual, ~11,000 non-synonymous single-nucleotide variants (SNVs) were detected and subsequently filtered for a minor allele frequency < 0.1% in in-house database comprising 7,000 control exomes and for biallelic variants assuming a recessive mode of inheritance. We identified 567, 14, and 13 genes in individuals #1-1, #2, and #3, respectively, carrying potentially biallelic variants with *NAXE* variants being identified in all three (Figure 3 and Table 1). The high number of variants in #1-1 reflects the African ancestry of this individual and limited efficacy of the frequency filter based on mainly Central European control subjects. In individual #1-1 we detected a homozygous c.177C>A (p.Tyr59*) variant, in individual #2 a compound heterozygous c.196C>T (p.Gln66*) and a 516+1G>A splice variant, and in individual #3 a homozygous c.804_807delinsA (p.Lys270del) variant. In individuals #2 and #3, *NAXE* was the only gene encoding a protein with a reported mitochondrial localization.¹⁰ In the 7,000 in-house control exomes, no other individual was found with predicted pathogenic biallelic variants in *NAXE*. For all three index case subjects, fibroblast cell lines were available for functional studies. Very recently, a fourth subject with a suspected mitochondrial disorder was exome

Table 1. Genetic and Clinical Findings in Individuals with Mutations in *NAXE*

NAXE Mutations			Clinical Features and Neuroimaging Findings							
ID	Sex	cDNA (NM_144772.2); Protein (NP_658985.2)	Age at Onset	Age at Death	Trigger at Initial Presentation	First Clinical Symptoms	Clinical Course	Cerebellar Edema/ Brain Herniation	Myelopathy on MRI	Skin Manifestations
#1-1	M	c.[177C>A];[177C>A]; p.[Tyr59*];[Tyr59*]	20 months	21 months	fever/infection	ataxia, torticollis, subacute tetraparesis, respiratory insufficiency	undulating disease course with episodes of stabilization, finally rapidly progressive with fatal outcome	yes	yes	yes
#1-2	F	ND	19 months	24 months	fever/infection	acute onset ataxia, subacute tetraparesis, respiratory insufficiency	undulating disease course with episodes of stabilization, finally rapidly progressive with fatal outcome	unclear	yes	yes
#2	F	c.[196C>T];[516+1G>A]; p.[Gln66*];[?]	15 months	24 months	fever/infection	delayed development, muscular hypotonia and nystagmus, sudden deterioration with respiratory failure	undulating disease course with episodes of stabilization, finally rapidly progressive with fatal outcome	yes	yes	yes
#3	M	c.[804_807delinsA];[804_807delinsA]; p.[Lys270del]; [Lys270del]	16 months	18 months	fever/infection	delayed development, muscular hypotonia, subacute-onset ataxia and nystagmus	rapidly progressive with fatal outcome	yes	ND	no
#4-1	M	c.[653A>T];[743delC]; p.[Asp218Val];[Ala248Glufs*26]	16 months	16 months	unclear	acute-onset ataxia, nystagmus, muscle hypotonia, dysarthria	undulating disease course with episodes of stabilization, finally rapidly progressive with fatal outcome	yes	ND	yes
#4-2	M	c.[653A>T];[743delC]; p.[Asp218Val];[Ala248Glufs*26]	8 months	28 months	unclear	delayed development, seizures, muscular hypotonia	undulating disease course with episodes of stabilization, finally rapidly progressive with fatal outcome	unclear	ND	no

Abbreviation is as follows: ND, not determined.

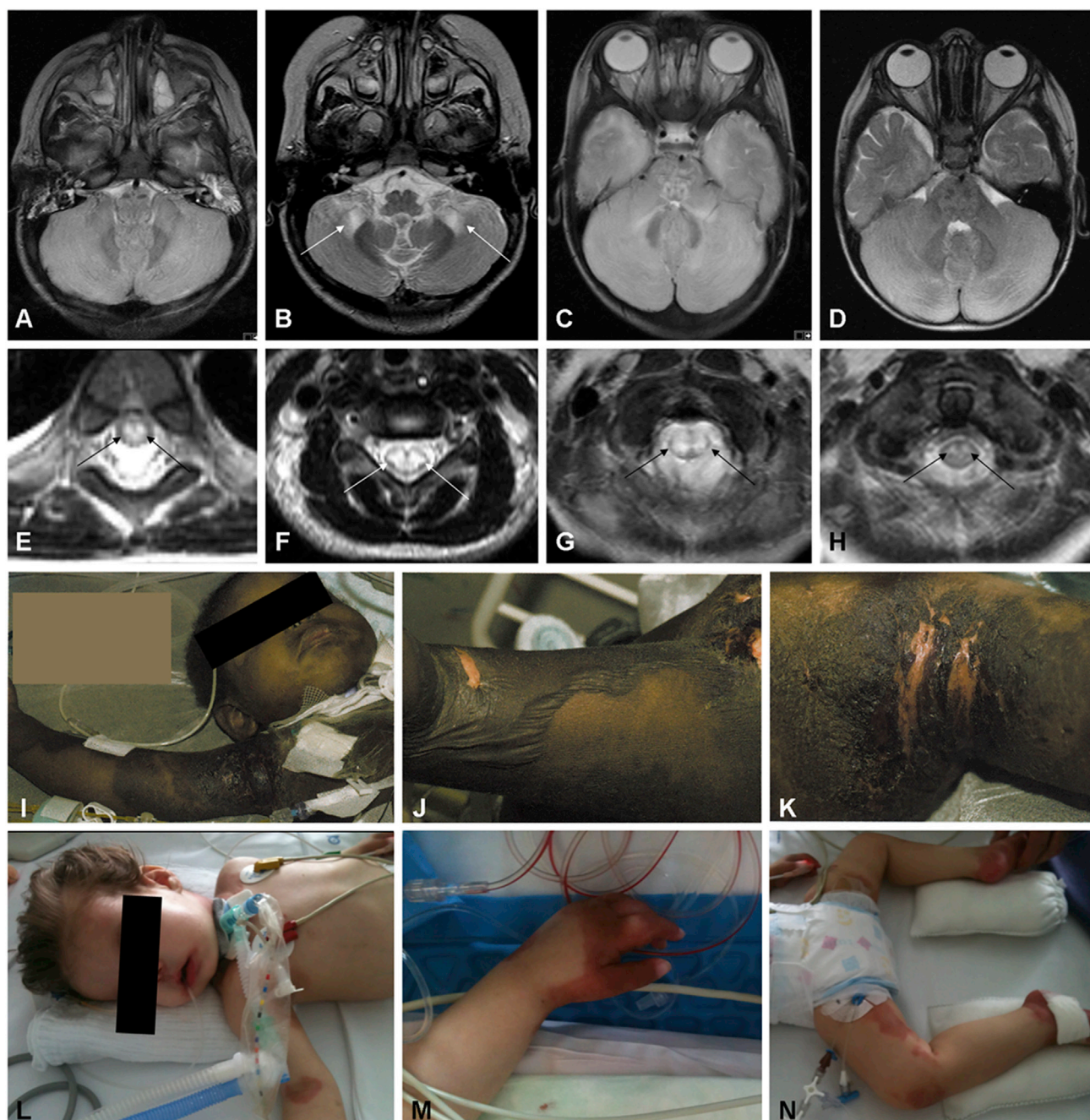


Figure 2. Unifying Neuroimaging Findings and Skin Manifestations in Children with *NAXE* Mutations

(A) Brain MRI (axial view, T2-weighted) of individual #1-1, showing diffuse cerebellar edema.

(B) Brain MRI of individual #1-2 (axial view, T2-weighted), demonstrating symmetrical signal alterations in cerebellar white matter and cerebellar peduncles.

(C) Brain MRI (axial view, T2-weighted) in individual #2 showing diffuse cerebellar edema comparable to the findings in (A), leading to nearly fatal brain herniation.

(D) Brain MRI (axial view, T2-weighted) of individual #4-1, also demonstrating diffuse cerebellar edema.

(E–H) Spinal MRI (axial view, T2-weighted) in individuals #1-1 (cervical spine) (E), #1-2 (thoracic spine) (F), #2 (cervical spine) (G), and #4-1 (cervical spine) (H), showing symmetrical signal abnormalities of the spinal cord, indicating various degrees of myelopathy. Please note that additional imaging findings can be found in [Figure S1](#).

(I–K) Extensive skin lesions in individual #1-2. Onset of skin manifestation was sub-acute within 2–3 weeks after the start of neurological symptoms. Large bullous skin lesions developed (J shows popliteal fossa), partially leading to erosion and eruption of the skin (K shows axilla).

(L–N) Skin lesions in individual #2.

Please also note the critical clinical condition of both affected individuals as indicated in (I) and (L).

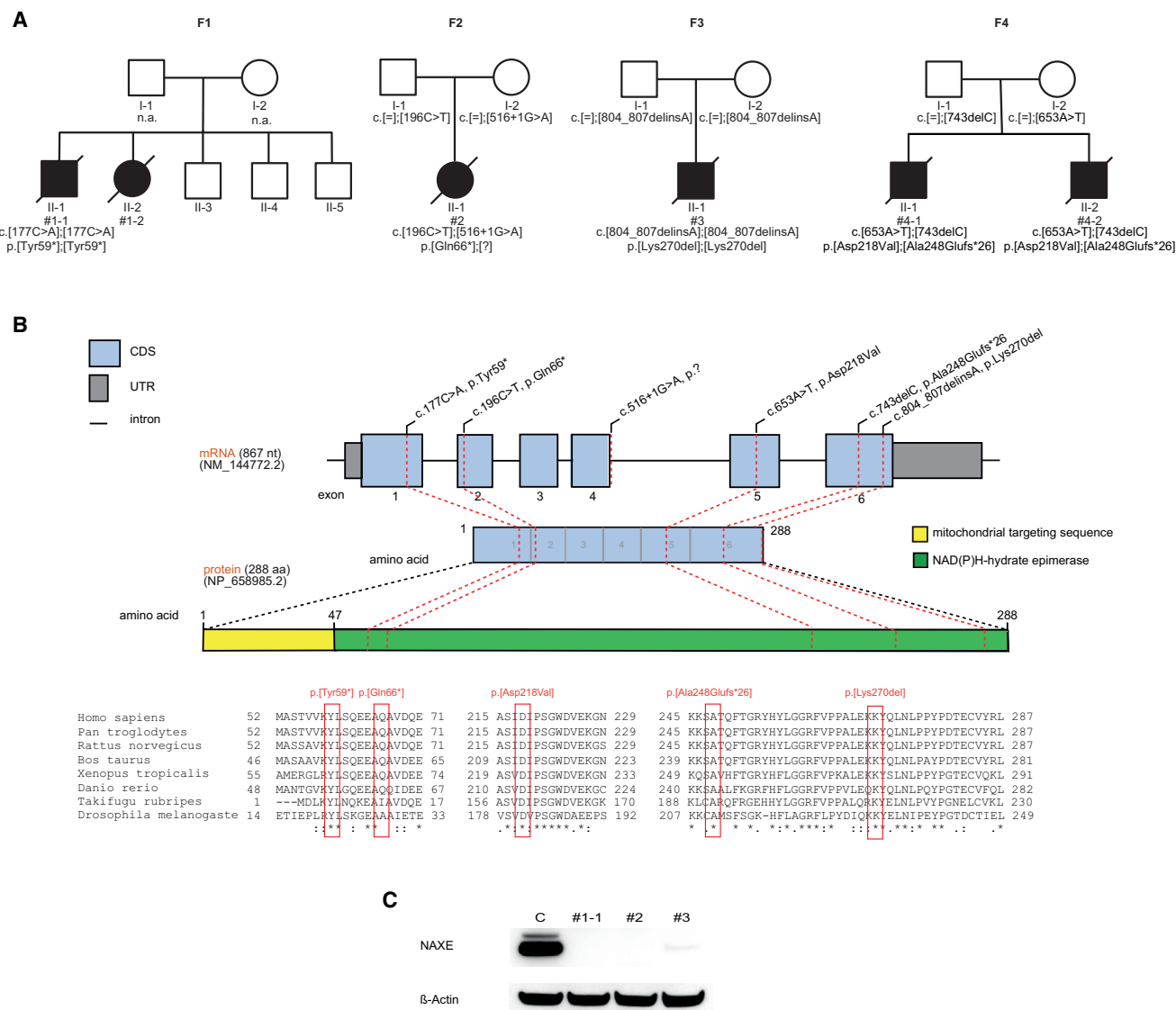


Figure 3. Genetic Findings in Four NAXE-Deficient Families with Consequences on the Protein Level

(A) Pedigrees of four families identified with recessive inherited mutations in *NAXE*.

(B) Genomic organization of *NAXE* with known conserved protein domains in the gene product, location of mutations within *NAXE*, and phylogenetic conservation of amino acid residues affected by mutations; positions of mutations are highlighted in red.

(C) Western blot analysis of fibroblast from index case subjects with *NAXE* mutations and a control cell line. Fibroblasts were cultured in Dulbecco's Modified Eagle's medium (Life Technologies) supplemented with 10% fetal bovine serum and 1% penicillin/streptomycin (both: Life Technologies) at 37°C in an atmosphere of 5% CO₂ in air. Whole cell lysates were prepared with cell lysis reagent CellLytic M (Sigma Aldrich). A polyclonal antibody against NAXE detecting amino acid sequence 218 to 286 (HPA048164, Sigma Aldrich) was used. A monoclonal antibody against beta-actin (Sigma Aldrich) served as loading control. Secondary antibodies were anti-mouse and anti-rabbit (GE Healthcare). Signal was detected using BM chemiluminescence blotting substrate (Roche).

sequenced in Poland. The library was prepared using the Nextera Rapid Capture Exome kit (Illumina) followed by sequencing as 2× 75 bp paired-end reads on the HiSeq1500 achieving on average 49-fold coverage, with 92.7% of the exome covered more than 10-fold. Data were processed as described.¹¹ In individual #4-1 a compound heterozygous frameshift (c.743delC) and missense mutation (c.653A>T) in *NAXE* was discovered (Figure 3). In this case, ~13,000 non-synonymous single-nucleotide variants (SNVs) were detected and subsequently filtered for variants with a minor allele frequency < 0.1% in both

in-house and public databases, identifying 147 variants. Filtering for predicted biallelic variants led to no identification of genes harboring variants in a homozygous state and only one gene harboring predicted pathogenic variants in a compound heterozygous state, *NAXE*.

The homozygous loss-of-function variant in individual #1-1, the homozygous deletion of Lys270 in individual #3, and the two variants found in individual #4-1 were absent from public databases. The c.196C>T (p.Gln66*) nonsense and c.516+1G>A splice variant detected in individual #2 were found four and one times

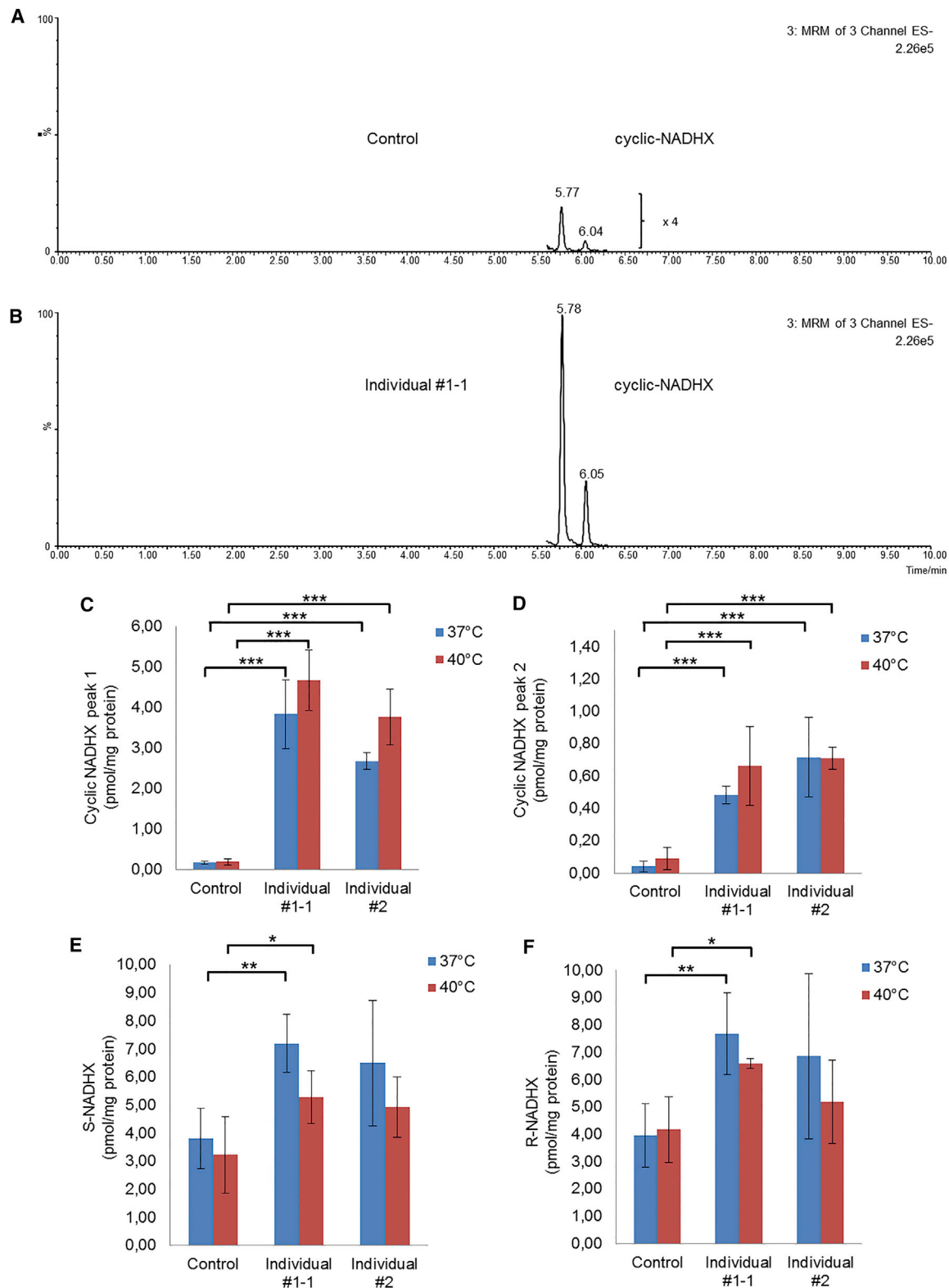


Figure 4. Cellular Consequences of NAXE Deficiency

(A and B) Typical examples of chromatograms of cyclic-NADHX analyzed by HPLC-ESI-MS/MS in a control cell line (A) and in the affected individual #1-1 (B). Chromatograms clearly show that the levels of cyclic-NADHX are increased in NAXE-deficient cells compared to controls. The two peaks that we measured for cyclic-NADHX most likely depict the R- and the S-form of the metabolite. In the control cell line (B), the peaks were additionally 4-fold magnified for better visualization.

(C and D) Quantitative results of the cyclic-NADHX measurements under normal (37°C) and heat-stressed (40°C) conditions for 24 hr.

(legend continued on next page)

only, respectively, in a heterozygous state in ~120,000 alleles of the Exome Aggregation Consortium (ExAC) Server (Cambridge, MA [09/2015]). All variants were confirmed by Sanger sequencing with parents being heterozygous carriers shown for families #2, #3, and #4.

Taken together, the identification of biallelic *NAXE* mutations in five individuals from four families with a strikingly similar phenotype establishes *NAXE* variants to be confidently implicated in this infancy-onset disease characterized by (sub-) acute-onset ataxia, cerebellar edema, spinal myelopathy, and skin lesions, induced by febrile infections, leading to coma and finally to death within the first 3 years of life.

Whereas the *NAXE* mutations found in individuals #1-1 and #2 are expected to result in a truncated protein being non-functional, the consequence of the Lys70 deletion on protein stability was unclear. Western blot analysis on fibroblasts derived from individuals #1, #2, and #3 revealed loss of *NAXE* in #1 and #2 and considerably reduced levels of *NAXE* in #3 (Figure 3). We therefore proceeded to use the fibroblast cell lines to study the consequences caused by the *NAXE* deficiency. Mutations in *NAXE* resulting in disrupted *NAXE* function are expected to impair the NAD(P)HX repair, which in turn should result in accumulation of the abnormal metabolites. We therefore measured levels of R-NADHX, S-NADHX, cyclic-NADHX, NAD, and NADH in fibroblast cell lines of two affected individuals and in two independent control cell lines. For optimization of the LC-MS/MS method, the compounds S-NADHX, R-NADHX, and cyclic-NADHX were synthesized from NADH under acidic pH conditions as published.⁶ Finally, for each individual sample, two T-75 cm² flasks containing fibroblasts (~90% confluency) were dissociated using TrypLE (Invitrogen) and cells were washed three times with ice-cold PBS. A portion of each sample was used for protein determination (BCA Protein Assay, Pierce). Next, cells were centrifuged at 300 × *g* and 4°C for 5 min. Stable isotope d4-nicotinamide was added as an internal standard prior to the ethanolic extraction procedure. Cell pellets were resuspended in 1 mL hot (80°C) 80% ethanol containing 20 mM HEPES (pH 7) and incubated at 80°C for 2 min followed by cooling on ice for 3 min. Next, cells were homogenized for 30 s using a Minilys homogenizer (Bertin). Samples were centrifuged at 15,000 × *g* and 4°C for 3 min. Supernatants were collected. For further use, a volume of 500 µL of the ethanolic extracts was gently dried under nitrogen stream. The dried sample was dissolved in 50 µL of 50 mM ammonium acetate (pH 7). After centrifugation, a volume of 30 µL was analyzed by HPLC-MS/MS system. The system consisted of an Acquity UPLC- I Class (Waters, UK) coupled to a Xevo TQ-S tandem mass spectrometer (Waters, UK) which is equipped with an ESI

source operating in the negative ion mode for the both epimers S- and R-NADHX, NADH, and cyclic-NADHX and in positive ion mode for NAD and d4-nicotinamide (internal standard). Quantitative data were conducted in the multiple reaction monitoring (MRM) mode. The chromatographic separation was performed on a Polaris 3 C18-A 150 × 2.0 mm HPLC column (Agilent) using acetonitrile and 50 mM ammonium acetate (pH 7) as mobile phases. A gradient elution mode was used for rapid separation of the analytes.

Target compounds were identified and quantified based on their retention times (4.47 min S-NADHX, 4.94 min R-NADHX, 5.34 min NADH, 5.79 and 6.07 min cyclic-NADHX, 4.78 min d4-nicotinamide, and 4.73 min NAD) and MS/MS fragments (664.1 > 158.8 *m/z*, 664.1 > 79 *m/z*, and 664.1 > 664.2 *m/z* for both NADH and cyclic-NADHX; 682.2 > 158.8 *m/z*, 682.2 > 79 *m/z*, and 682.2 > 682.1 *m/z* for both epimers S-NADHX and R-NADHX; 127.1 > 84.1 *m/z* for d4-nicotinamide; 664.1 > 136.1 *m/z* and 664.1 > 427.8 *m/z* for NAD).

Fibroblasts with loss-of-function mutations in *NAXE* showed a significant increase in cyclic-NADHX levels compared to controls (Figure 4). Upon heat stress, we observed a further gradual increase in *NAXE*-deficient cells. The levels of R-NADHX and S-NADHX were also increased, but to a lesser extent than observed for cyclic-NADHX. The levels of NAD and NADH were not significantly altered (data not shown).

Toxic metabolites or damaged cofactors can occur due to instability of cellular substances or (undesirable) moonlighting reactions of enzymes. To avoid the accumulation of such metabolites and to prevent cellular damage, “support systems” dedicated to metabolite repair have developed during evolution.¹ The clinical importance of such systems was mostly unnoticed until the first inherited metabolic diseases related to deficient repair enzymes were described (e.g., D-2-hydroxyglutaric aciduria type II¹² [MIM: 613657]). These studies highlighted the importance of metabolite repair systems for mammalian development and viability. Here, the identification of six individuals with a strikingly uniform clinical phenotype with biallelic *NAXE* variants in four families, including two homozygous loss-of-function variants, establishes *NAXE* variants as cause of a human disease of metabolite repair. *NAXE* is an essential component of the NAD(P)HX repair system. Its deficiency causes a detectable accumulation of the toxic metabolite cyclic-NADHX, which has been shown to inhibit various cellular NADH dehydrogenases.^{3,13} The inhibition of NADH dehydrogenases is therefore a likely pathomechanism of *NAXE* deficiency. The decreased activity of complex I (MIM: 252010) and pyruvate oxidation in the investigation of intact

(E and F) Quantitative results of S- and R-NADHX measurements. Control bar graphs depict pooled data obtained from two independent healthy cell lines.

All experimental data were obtained in at least three independent experiments. Student's *t* test was used to determine the statistical significance. Statistics: ****p* < 0.001, ***p* < 0.01, and **p* < 0.05 relative to controls. Error bars indicate standard deviation.

mitochondria from fresh muscle biopsies of individuals #1-1 and #3 (Table S1) support this hypothesis.

NADH and NADPH are major cofactors of biochemical reactions with more than 250 entries in the Uniprot database for enzymes in human metabolism that rely on one of these two cofactors. These reactions are localized in all parts of the cell, many of them are found in mitochondria, especially those with high turnover rates. Elevated lactate levels in cerebrospinal fluid, as found in all *NAXE*-deficient individuals, are suggesting a deficiency/disturbance in mitochondrial energy metabolism. Reduced activities in intact mitochondria found in muscle biopsies of individuals #1-1 and #3 also indicate the pathogenic effects of *NAXE* mutations on the mitochondrial oxidative phosphorylation.

Of note, disturbed NAD metabolism as a cause of human disease is not entirely novel. The best-known condition is certainly pellagra,¹⁴ an acquired condition caused by a chronic lack of nicotinic acid (vitamin B3). In view of the skin manifestations in our affected individuals, it is tempting to speculate about similarities in the underlying pathomechanisms. However, skin lesions in our individuals were not typically located (e.g., not primarily affecting sun-exposed areas), appeared bullous/Lyell-like (e.g., not scaly or desquamating), and neurological (especially cerebellar) signs were dominating the clinical picture.

An inherited disorder indirectly affecting NAD metabolism is the so-called Hartnup disease (MIM: 234500).¹⁵ The disorder is caused by mutations in *SLC6A19* (MIM: 608893), which encodes the sodium-dependent neutral amino acid transporter B(0)AT1.¹⁶ The defect impairs the absorption of neutral amino acids like tryptophan, which further serves as an important precursor in the biosynthesis of nicotinic acid in humans. Strikingly, Hartnup disease is characterized by a pellagra-like light-sensitive rash in combination with cerebellar ataxia. In addition to classical Hartnup disease, other “pellagra-like” conditions (MIM: 260650) have also been described. Freundlich et al.¹⁷ and Salih et al.¹⁸ both reported about familial disorders with pellagra-like skin lesions associated with neurologic abnormalities and cerebellar symptoms (MIM: 260650). Also in these disorders, a disturbance of tryptophan metabolism was suggested. In contrast to Hartnup disease, these disorders had an onset in early childhood and were lethal in most of the cases (one child described by Freundlich et al. died at the age of 15 months; none of the ten affected children described by Salih et al. survived beyond 2 years of age).^{17,18} Interestingly, one of the three affected individuals reported by Freundlich et al. had a milder phenotype and symptoms of pellagra first at the age of 4 years, which could be successfully treated by nicotinamide. He experienced several crises with pellagra but also combined with ataxia and even with coma at the age of 14 years, but he recovered with nicotinamide treatment (100 mg/day).¹⁷ These findings suggest similarities to the disorder reported here. The reason for the cerebellar/neurological symptoms in

Hartnup disease and associated conditions is still enigmatic. It was speculated whether a reduced synthesis of 5-hydroxytryptamine in the nervous system or the production of an abnormal by-product in tryptophan degradation pathway might be responsible for the neurological problems.^{17,18}

Importantly, in classical pellagra as well as in the inherited pellagra-like conditions, administration of nicotinic acid has a therapeutic effect.^{14,17,18} Therefore, it is tempting to speculate whether nicotinic acid supplementation might be beneficial in affected individuals with *NAXE* mutations. Further in vitro studies will be required to investigate this potential treatment strategy.

In general, early fever control might be beneficial in affected individuals. Intriguingly, in all children reported here, onset of symptoms and/or clinical deterioration was triggered by infections with high fever. This observation gains importance in view of evidence from basic research, indicating that NADPHX especially arises at high temperatures or acidic pH.² Accordingly, in our cell studies, we also observed a gradual increase of cyclic-NADHX levels after *NAXE*-deficient cells were exposed to heat stress. In that respect, early and sustained antipyretic therapy might help to mitigate metabolic decompensation in *NAXE*-deficient individuals and should be accompanied by general supportive measures (e.g., adequate caloric supply, infusion therapy, etc.). Importantly, because of the combination of high fever and acute neurological deterioration, encephalitis, meningitis, or autoimmune-mediated inflammation was initially suspected in the children. Our findings suggest that *NAXE* deficiency should be considered as an important differential diagnosis in such cases. Additional evidence is provided by a report that was published during the review process of this article. The authors describe a family with five affected siblings with a similar clinical presentation as described here and biallelic variants in *NAXE*.¹⁹

In summary, we describe a disorder of metabolite repair, placing great importance to safeguarding the cell from the accumulation of potentially harmful metabolic intermediates. A defective NAD(P)HX repair system resulted in elevated concentrations of toxic cyclic-NADHX along with rapidly progressive ataxia, spinal myelopathy, skin lesions, and cerebellar edema leading to coma and finally to death within the first 3 years of life.

Supplemental Data

Supplemental Data include detailed case reports, one figure and one table and can be found with this article online at <http://dx.doi.org/10.1016/j.ajhg.2016.07.018>.

Acknowledgments

We thank all families for their participation and for providing important samples for the present research study. For their work on individual #3, we thank Mrs. Ira Brandstetter (mitochondrial

respiratory chain biochemistry), Mrs. Julia Emmerich (fibroblast isolation from muscle biopsy), and Dr. Benedikt Schoser (assessment of muscle morphology and ultrastructure). We thank Prof. Marjo van der Knaap for the assessment of the MRI from individual #2. The study was supported by the German Bundesministerium für Bildung und Forschung (BMBF) through the German Network for mitochondrial disorders (mitoNET, 01GM1113A-E to L.S.K., K.D., W.M.-F., T.M., T.K., J.A.M., F.D., and H.P.), the E-Rare project GENOMIT (01GM1603 to J.A.M. and H.P.), the Juniorverbund in der Systemmedizin “mitOmics” (FKZ 01ZX1405C to T.B.H.), and the Forschungskommission of the Medical Faculty of the Heinrich-Heine-University Düsseldorf (F.D. and K.D.). This study was further supported by the CMHI project S136/13.

Received: January 15, 2016

Accepted: July 14, 2016

Published: September 8, 2016

Web Resources

ExAC Browser, <http://exac.broadinstitute.org/>

GenBank, <http://www.ncbi.nlm.nih.gov/genbank/>

OMIM, <http://www.omim.org/>

UniProt, <http://www.uniprot.org/>

References

- Linster, C.L., Van Schaftingen, E., and Hanson, A.D. (2013). Metabolite damage and its repair or pre-emption. *Nat. Chem. Biol.* 9, 72–80.
- Yoshida, A., and Dave, V. (1975). Inhibition of NADP-dependent dehydrogenases by modified products of NADPH. *Arch. Biochem. Biophys.* 169, 298–303.
- Marbaix, A.Y., Tyteca, D., Niehaus, T.D., Hanson, A.D., Linster, C.L., and Van Schaftingen, E. (2014). Occurrence and subcellular distribution of the NADPHX repair system in mammals. *Biochem. J.* 460, 49–58.
- Marbaix, A.Y., Noël, G., Detroux, A.M., Vertommen, D., Van Schaftingen, E., and Linster, C.L. (2011). Extremely conserved ATP- or ADP-dependent enzymatic system for nicotinamide nucleotide repair. *J. Biol. Chem.* 286, 41246–41252.
- Giaever, G., Chu, A.M., Ni, L., Connelly, C., Riles, L., Véronneau, S., Dow, S., Lucau-Danila, A., Anderson, K., André, B., et al. (2002). Functional profiling of the *Saccharomyces cerevisiae* genome. *Nature* 418, 387–391.
- Niehaus, T.D., Richardson, L.G., Gidda, S.K., ElBadawi-Sidhu, M., Meissen, J.K., Mullen, R.T., Fiehn, O., and Hanson, A.D. (2014). Plants utilize a highly conserved system for repair of NADH and NADPH hydrates. *Plant Physiol.* 165, 52–61.
- Haack, T.B., Haberberger, B., Frisch, E.M., Wieland, T., Iuso, A., Gorza, M., Strecker, V., Graf, E., Mayr, J.A., Herberg, U., et al. (2012). Molecular diagnosis in mitochondrial complex I deficiency using exome sequencing. *J. Med. Genet.* 49, 277–283.
- Haack, T.B., Kopajtich, R., Freisinger, P., Wieland, T., Rorbach, J., Nicholls, T.J., Baruffini, E., Walther, A., Danhauser, K., Zimmermann, F.A., et al. (2013). ELAC2 mutations cause a mitochondrial RNA processing defect associated with hypertrophic cardiomyopathy. *Am. J. Hum. Genet.* 93, 211–223.
- Li, H., and Durbin, R. (2009). Fast and accurate short read alignment with Burrows-Wheeler transform. *Bioinformatics* 25, 1754–1760.
- Elstner, M., Andreoli, C., Ahting, U., Tetko, I., Klopstock, T., Meitinger, T., and Prokisch, H. (2008). MitoP2: an integrative tool for the analysis of the mitochondrial proteome. *Mol. Biotechnol.* 40, 306–315.
- Ploski, R., Pollak, A., Müller, S., Franaszczyk, M., Michalak, E., Kosinska, J., Stawinski, P., Spiewak, M., Seggewiss, H., and Bilinska, Z.T. (2014). Does p.Q247X in TRIM63 cause human hypertrophic cardiomyopathy? *Circ. Res.* 114, e2–e5.
- Kranendijk, M., Struys, E.A., van Schaftingen, E., Gibson, K.M., Kanhai, W.A., van der Knaap, M.S., Amiel, J., Buist, N.R., Das, A.M., de Klerk, J.B., et al. (2010). IDH2 mutations in patients with D-2-hydroxyglutaric aciduria. *Science* 330, 336.
- Prabhakar, P., Laboy, J.I., Wang, J., Budker, T., Din, Z.Z., Chobanian, M., and Fahien, L.A. (1998). Effect of NADH-X on cytosolic glycerol-3-phosphate dehydrogenase. *Arch. Biochem. Biophys.* 360, 195–205.
- Hegyi, J., Schwartz, R.A., and Hegyi, V. (2004). Pellagra: dermatitis, dementia, and diarrhea. *Int. J. Dermatol.* 43, 1–5.
- Baron, D.N., Dent, C.E., Harris, H., Hart, E.W., and Jepson, J.B. (1956). Hereditary pellagra-like skin rash with temporary cerebellar ataxia, constant renal amino-aciduria, and other bizarre biochemical features. *Lancet* 271, 421–428.
- Kleta, R., Romeo, E., Ristic, Z., Ohura, T., Stuart, C., Arcos-Burgos, M., Dave, M.H., Wagner, C.A., Camargo, S.R., Inoue, S., et al. (2004). Mutations in SLC6A19, encoding B0AT1, cause Hartnup disorder. *Nat. Genet.* 36, 999–1002.
- Freundlich, E., Statter, M., and Yatziv, S. (1981). Familial pellagra-like skin rash with neurological manifestations. *Arch. Dis. Child.* 56, 146–148.
- Salih, M.A., Bender, D.A., and McCreanor, G.M. (1985). Lethal familial pellagra-like skin lesion associated with neurologic and developmental impairment and the development of cataracts. *Pediatrics* 76, 787–793.
- Spiegel, R., Shaag, A., Shalev, S., and Elpeleg, O. (2016). Homozygous mutation in the APOA1BP is associated with a lethal infantile leukoencephalopathy. *Neurogenetics* 17, 187–190.

Supplemental Data

***NAXE* Mutations Disrupt the Cellular NAD(P)H**

Repair System and Cause a Lethal

Neurometabolic Disorder of Early Childhood

Laura S. Kremer, Katharina Danhauser, Diran Herebian, Danijela Petkovic Ramadza, Dorota Piekutowska-Abramczuk, Annette Seibt, Wolfgang Müller-Felber, Tobias B. Haack, Rafał Płoski, Klaus Lohmeier, Dominik Schneider, Dirk Klee, Dariusz Rokicki, Ertan Mayatepek, Tim M. Strom, Thomas Meitinger, Thomas Klopstock, Ewa Pronicka, Johannes A. Mayr, Ivo Baric, Felix Distelmaier, and Holger Prokisch

Supplemental Case Reports

Individual #1-1 (c.[177C>A];[177C>A]; p.[Tyr59*];[Tyr59*]), a boy, was born to healthy consanguineous parents from Gambia. Among his siblings, one girl was similarly affected (Individual #1-2, see below), one was a premature infant who died at the age of three months, and three are healthy. The index case was considered normal at birth (birth weight 3540 g, lengths 55 cm) and medical follow-up during the first 1.5 years of life was unremarkable. In particular, no neurological problems or developmental delay were noted.

At the age of 20 months, he suffered from a febrile tonsillitis (temperatures up to 40°C), which was treated with oral antibiotics. Shortly after the start of fever, he developed a torticollis and was admitted to the hospital. Initial examination additionally revealed ataxia. He received intravenous fluids and antibiotics. An initial brain MRI was without obvious pathological findings. During the following days his situation gradually improved. However, about two weeks after admission, the boy again developed fever and his neurological status deteriorated with severe ataxia and nystagmus. In the following, he suddenly suffered from respiratory insufficiency, requiring intensive care treatment and mechanical ventilation. Brain MRI showed severe cerebellar edema and spinal MRI revealed extensive myelopathy (see Figure 2 as well as Figure S1). Laboratory investigations of blood and cerebrospinal fluid demonstrated transiently elevated lactate levels (in blood up to 4.6 mmol/L, NR <1.6; in CSF up to 2.69 mmol/L, NR <2.24 mmol/L). Extensive metabolic, immunological, and microbiological investigations were without any specific findings. During the further course, the boy developed massive Lyell-like bullous skin lesions of unclear aetiology. Under the suspicion of a mitochondrial disorder, a muscle and skin biopsy was performed. Biochemical examination of fresh muscle tissue revealed mild

mitochondrial complex I deficiency (64 mU/U citrate synthase [CS]; NR 70-251 mU/U CS) and a globally reduced ATP production rate (15.5 nmol/h.mU CS; NR 42.1-81.2 nmol/h.mU CS). Investigation of skin fibroblasts was normal. During the further clinical course the boy was comatose und suffered from repeated seizures. Finally, at the age of 21 month he died due to cardiovascular failure.

Individual #1-2, a girl, was born as the third child of the parents. As described for her brother (individual #1-1), pregnancy, birth and postnatal development were unremarkable.

At the age of 19 months, the child suffered from a febrile respiratory infection (temperatures up to 39.9 °C). Two days after onset of symptoms her clinical condition deteriorated. She vomited repeatedly and developed ataxia. Despite emergency hospital admission and application of intravenous fluids as well as antibiotics neurological signs were rapidly progressive and the girl developed a flaccid tetraparesis, requiring mechanical ventilation. Brain MRI demonstrated symmetrical signal alterations of cerebellar white matter and spinal MRI revealed extensive myelopathy (C2-Th10; see Figure 2). Laboratory investigations showed transiently elevated liver enzymes (GOT up to 790 U/L, NR <52 U/L; GPT up to 785 U/L, NR <29 U/L). Analysis of cerebrospinal fluid revealed moderately increased lactate levels (up to 3.2 mmol/L, NR <2.24 mmol/L). Immunological, microbiological and viral investigations were without specific findings. Under the suspicion of an autoimmune disease (e.g. transverse myelitis), intravenous cortisone and immunoglobulins were administered without therapeutic effect. About 14 days after onset of neurological signs, transient ichthyosiform skin changes were noted mainly at the abdomen and the inguinal region.

For the next 2 months, the child was continuously treated at the intensive care unit and required mechanical ventilation. However, her condition was rather stable and even slightly improved until she suddenly developed fever, abdominal distension and repeated seizures. In addition, massive Lyell-like bullous skin lesions developed as observed in her brother (see Figure 2). A skin biopsy was taken, which showed intraepidermal bullae without signs of inflammation. Based on the histology results, a staphylococcal Lyell's syndrome or a toxic epidermal necrolysis appeared to be unlikely. The neurological status of the girl further deteriorated, and examination revealed absence of pupil reactions to light, of pharyngeal and tracheal reflexes and of spontaneous breathing. Follow-up MRI demonstrated severe global brain atrophy (see Figure S1). While mechanical ventilation was sustained, she finally died at the age of 24 months due to cardiovascular failure. Autopsy was performed after parental consent and revealed extensive areas of necrosis affecting brain stem, as well as cervical and thoracic spine.

Individual #2 (c.[196C>T];[516+1G>A]; p.[Gln66*];[?]), a girl, was born as the first child of healthy and unrelated parents in Croatia. A previous pregnancy of the mother had ended by early miscarriage of unknown cause. The index case was born on term, after normal pregnancy and uneventful delivery (birth weight 3740 g, lengths 48 cm). Development was normal until the second half of the first year when she failed to thrive and had mild psychomotor delay. Parents also reported fatigue, occasional tremor and convergent strabismus, which were more pronounced after exertion. At the age of 15 months the child experienced psychomotor regression during febrile illness, but fully recovered during the following few weeks.

At the age of 17 months she had respiratory infection with high fever. On the third day of illness, acute deterioration with respiratory failure occurred. She was resuscitated in hospital and had normal oxygenation and heart rate during the whole process. Upon admission to hospital her GCS was 8, blood gases, CBC, glucose, electrolytes, aminotransferases, urea, creatinine, CK and protein electrophoresis were normal. CSF lactate was high (4.1 mmol/L; NR < 2.2 mmol/L), other CSF findings (cells, proteins, glucose) were normal and blood lactate was slightly increased (1.9 mmol/L; NR < 1.33). Metabolic work-up (plasma and CSF amino acids, organic acids in urine) was unremarkable except for mildly increased excretion of pyruvate in urine. Electroencephalogram showed slower brain activity (4-5 Hz), but without epileptic discharges. Brain MRI showed extensive signal abnormalities in the cortex, subcortical cerebral white matter, caudate nucleus, putamen, pons, middle cerebellar peduncles and medulla oblongata. Moreover, cerebellar edema and cervical myelopathy were seen (Figure 2). Diffusion-weighted images showed diffusion restriction in large areas of the cerebral cortex. Due to clinical presentation and symmetrical basal ganglia involvement, treatment with a mitochondrial cocktail was started (L-arginine, coenzyme Q10, vitamins C, B1 and B2). Muscle biopsy showed myopathic changes, while respiratory chain enzyme and pyruvate dehydrogenase activities in fresh frozen muscle were normal. During the following month she was in coma and had tracheostomy. After one month of mechanical ventilation she was successfully weaned from ventilator. At that point she reacted on painful stimuli, but still had disturbed consciousness with hyperkinesia of face muscles, extremity tremor, nystagmus and rigidity of upper limbs. Control MRI performed in one month intervals showed global brain atrophy with thin cerebral cortex, reduced white matter and signal abnormalities in the caudate nucleus and

putamen. The brainstem and cerebellum were relatively preserved (Figure 2 and Figure S1). Since thiamine transporter deficiency was suspected, thiamine was increased to 200 mg bid per day (previously 100 mg), biotin was added to the cocktail, and antiepileptic treatment was modified (clonazepam for the treatment of hyperkinesia), thereafter she markedly improved. In the following days hyperkinesia almost disappeared, she started to fixate objects and respond to her parents. During the next weeks her muscle tone was improved and she could sit unsupported. About three months after first crisis, her condition worsened again, she became hypotonic with more pronounced strabismus, tremor and psychomotor restlessness. She had short episodes of fever, and erythematous rash on intertriginous and perigenital areas, hands, and feet. MRI performed at that point showed thin cerebral cortex with diffusely abnormal signal, cerebral white matter atrophy, and mild signal abnormalities in the caudate nucleus and putamen. MRS showed increased choline and mildly increased lactate in deep white matter and normal metabolite peaks in basal ganglia. Soon, she again developed respiratory insufficiency and a deep coma from which she never recovered. CT scan revealed hypodensity of mesencephalon, pons, and medulla oblongata with brain edema, herniation of cerebellar tonsils with enlarged IV ventricle and hypertensive hydrocephalus. External ventricular drain was placed. CSF lactate was elevated (5.0 mmol/L; NR < 2.2 mmol/L) while blood lactate was normal or close to normal. In the following days skin changes worsened and she had sharply demarcated edematous and erythematous rash on feet, hands, limbs, and areas around mouth and eyes (Figure 2). Skin biopsy showed focal keratosis and normal dermis without inflammation. Clinically, she had signs of systemic inflammatory reaction. Immunological and microbiological work-up was unremarkable. She received intravenous immunoglobulins (2g/kg) and pulse doses of

steroids but there was no obvious benefit. She lost all her hair. After the skin peeled off the skin changes resolved. Further clinical course was complicated with *C. difficile* colitis and sepsis. Control brain MRI three weeks after deterioration showed diffuse brain edema, especially in cerebellum and brain stem as well as cervical myelopathy (Figure 2). After 6 weeks ventricular drainage was taken out and there was no need to place ventriculoperitoneal shunt. Further course was complicated by episodes of hemodynamic instability probably of central origin and sepsis. Last brain MRI was performed two months after deterioration and showed diffuse atrophy, reduced diffusion due to cytotoxic edema of brain stem and cerebellar white matter, and extensive cystic alterations of pons, cerebellar peduncles, pontomesencephalic and pontomedullary junctions. The girl died at the age of 24 months due to sepsis which led to irreversible circulatory failure. Autopsy showed periventricular and cortico-subcortical encephalomalacia with massive brain edema.

Individual #3 (c.[804_807delinsA];[804_807delinsA]; p.[Lys270del];[Lys270del]), a boy, was born after normal pregnancy and labor at 41 weeks of gestational age (birth weight 3510 g) in Germany. He had a mild developmental delay. He was able to crawl at 10 months. He started to sit at 11 months and remained slightly unstable when sitting. At 12 months he was able to speak single words.

At the age of 16 months he developed a bilateral ptosis, a left-sided abducens palsy and a vertical gaze palsy. To exclude a myasthenic syndrome, an edrophonium test was done which was negative and the boy was hospitalized for further diagnostic workup. Three days after admission to the hospital he showed progressive ataxia of trunk and limbs as well as an upgaze nystagmus. Tendon reflexes were normal, and there was no central paresis. He was irritable but mental function was otherwise

normal. He had a mild upper respiratory tract infection. Brain MRI was normal. Ventricles were not enlarged and there was no increased signal intensity in basal ganglia or brain stem. Metabolic screening (organic acids in urine, amino acids in plasma and CSF, carnitine and acylcarnitines) were normal. Nerve conduction velocities were in the normal range. Following anesthesia for the MRI the child remained very sleepy. At day 8 he became progressively somnolent. CSF examination showed an increase of lactate (3.6 mmol/L) but was otherwise normal (cells, protein, glucose). In the following night high fever (39.9°C), central bradypnea, and coma (GCS 4-6) developed. At admission to the ICU, blood gases were normal, but 2 hours later he showed progressive respiratory failure with a pCO₂ of 59 mm Hg and he was intubated. A thorax scan showed signs of beginning pneumonia. On day 11, a CT scan of the brain showed severe brain edema with absent grey and white matter differentiation, beginning herniation of the cerebellum but widely enlarged ventricles I, II and III. Histological, histochemical and ultrastructural examination of a vastus lateralis muscle biopsy was largely normal but showed some lipid and glycogen accumulation as well as aggregated mitochondria without paracrystalline inclusions in single fibers. Functional investigation of intact mitochondrial from a fresh muscle biopsy showed decreased oxidation of pyruvate-containing substrates while acetylcarnitine substrates were normally oxidized (Table S1). Complexes I –V of the oxidative phosphorylation and pyruvate dehydrogenase had normal activity. On day 12 pupils dilated and became unresponsive. The child died 12 days after admission.

Individual #4-1 (c.[653A>T];[743delC]; p.[Asp218Val];[Ala248Glufs*26]), a boy, was born after uneventful pregnancy and labor at 38 weeks of gestational age (birth weight was 3100 g) in Poland. His neonatal and infantile period was uneventful. At

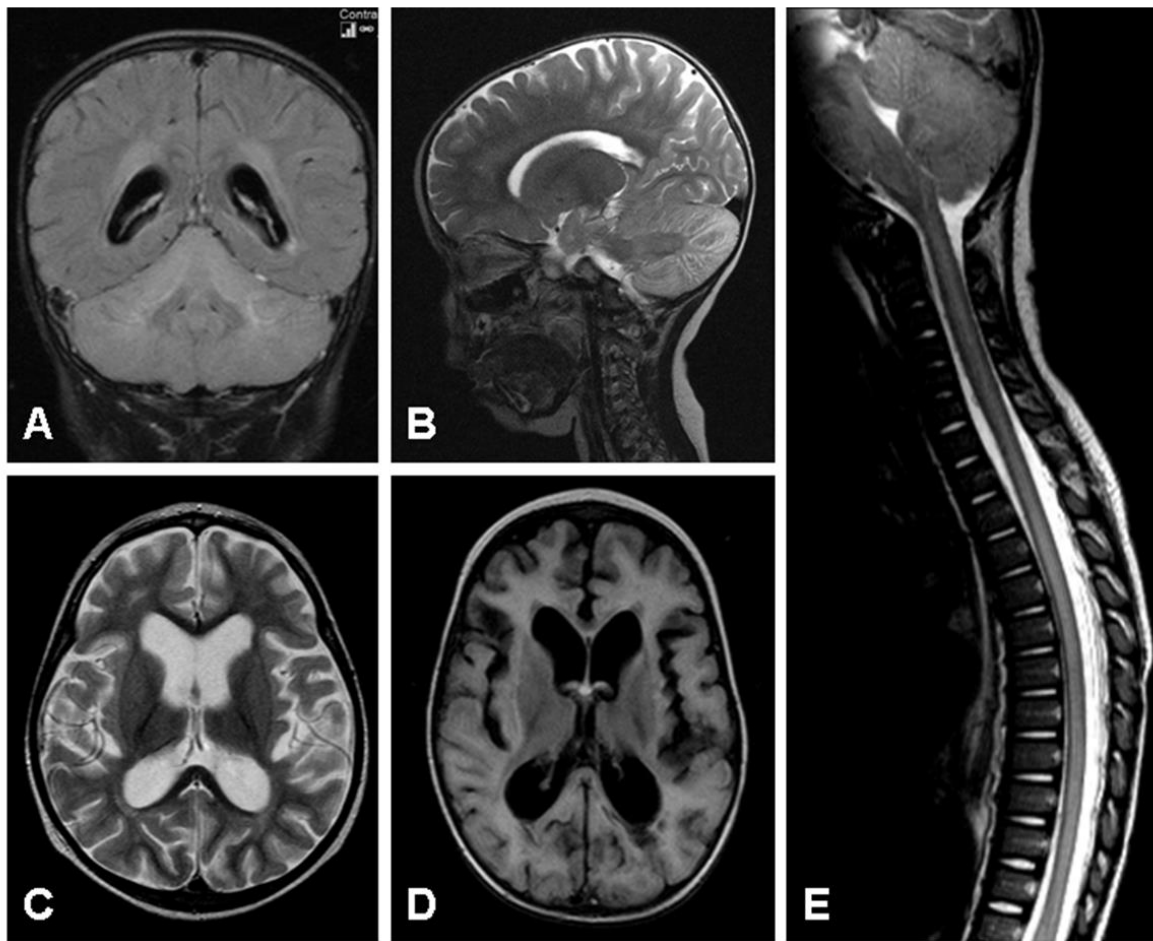
the age of 16 months he presented with an acute episode of ataxia. Emergency CT scan was without obvious pathology. Lumbar puncture was performed and CSF analysis was normal, although lactate was slightly elevated (2.6 mmol/L, NR < 2.2 mmol/L). Ataxia resolved after 3 weeks of steroid treatment. The next episode of ataxia occurred at the age of 29 months, with nystagmus, muscle hypotonia, and dysarthria. Brain MRI showed no pathologies. Electroencephalogram showed diffuse and slow activity (2.7-5 Hz). Lactate in CSF was 3.7 mmol/L (NR < 2.2 mmol/L). This time, disease progressed quickly. Two days after beginning of symptoms the boy became comatose, and developed respiratory insufficiency due to bradypnea. He required intubation and mechanical ventilation. After 7 days the child was still in coma. Electroencephalogram showed diffuse slow waves (1.5-2 Hz, 160-400 μ V). One focal reddish, psoriatic skin change on neck was observed. MRI of the brain revealed severe cerebellum and brain stem edema with T2 hypo/hyperintense changes in cerebellum and the cervical spine (see Figure 2 and Figure S1). Intensive antiedema therapy was introduced without clinical improvement. As the disease resembled acute viral encephalitis, virological tests were performed, which were negative, as well as were metabolic tests. Level of protein in CSF was normal. On the 14th day of the episodes CT scan revealed massive brain edema and isoelectric line in electroencephalogram was found. The next day the child died. Autopsy showed massive brain edema and lack of Purkinje cells in cerebellum.

Individual #4-2 (c.[653A>T];[743delC]; p.[Asp218Val];[Ala248Glufs*26]) the brother of individual #4-1, was born after uneventful pregnancy at 41 weeks of gestational age (Birth weight 3190 g). His psychomotor development was delayed due to muscular hypotonia.

At the age of 8 months he presented with myoclonic seizures, which were treated with valproate (VLP). He developed transient respiratory insufficiency requiring mechanical respiratory support. Later he was discharged home with gradual clinical improvement. After rehabilitation therapy and withdrawal of VLP he began to walk with support. At the age of 20 months the boy developed a further episode of acute deterioration. He rapidly became hypotonic, comatose and again suffered from seizures. Disease progressed and during one week he developed coma, respiratory insufficiency and acute hydrocephalus, requiring a ventriculoperitoneal shunt. In CSF increased lactate levels were found. Consecutive CT scans revealed progressive brain atrophy, especially of the brain stem. The child died at the age of 24 months, after 4 months hospitalization and intensive care treatment.

SUPPLEMENTAL FIGURES

Figure S1. Additional neuroimaging findings in patients with *NAXE* mutations



A) Brain MRI (coronal view, T2-weighted) of individual #1-1, showing diffuse cerebellar edema. B) Brain MRI (sagittal view, T2-weighted) of individual #4-1, demonstrating diffuse signal abnormalities and edema of the cerebellum. C) Brain MRI (axial view, T2-weighted) of individual #1-2 after several months after onset of symptoms showing severe global brain atrophy. D) Brain MRI (axial view, T2 TIRM dark fluid) of individual #2 after long term intensive care treatment showing a similar degree of brain atrophy as seen in C). E) Spinal MRI (sagittal view, T2-weighted) of patient 1-2 demonstrating affection of nearly the complete spinal cord.

SUPPLEMENTAL TABLES

Table S1. Biochemical analysis in muscle biopsy of individual #3

<i>I. Enzyme investigations</i>	mUnit/mg protein	mUnit/mUnit CS
Citrate synthase (CS)	95 (150 - 338)	
Complex I	24 (28 - 76)	0,25 (0,14 - 0,35)
Complex I+III	63 (49 - 218)	0,67 (0,24 - 0,81)
Complex II	18 (33 - 102)	0,19 (0,18 - 0,41)
Complex II+III	34 (65 - 180)	0,36 (0,3 - 0,67)
Complex III	164 (304 - 896)	1,73 (1,45 - 3,76)
Cytochrome c oxidase	190 (181 - 593)	2,00 (0,91 - 2,24)
Complex V	90 (86 - 257)	0,95 (0,42 - 1,26)
Pyruvate dehydrogenase	8,3 (5,3 - 19,8)	0,087 (0,026 - 0,079)
<i>II. Substrate oxidation</i>	nmol/h/mg protein	nmol/h/mUnit CS
[1-14C]Pyruvate+malate	122 (263 - 900)	1,29 (1,54 - 3,55)
[1-14C]Pyruvate+carnitine	139 (302 - 856)	1,47 (1,65 - 3,66)
[U-14C]Malat+pyruvate+malonate	132 (282 - 874)	1,40 (1,56 - 3,87)
[U-14C]Malat+acetylcarn.+malonate	165 (273 - 678)	1,74 (1,16 - 2,82)
[U-14C]Malat+acetylcarn.+arsenite	83 (156 - 378)	0,88 (0,57 - 1,52)
[U-14C]Glutamat+acetylcarnitine	34 (86 - 209)	0,36 (0,35 - 1,06)

normal ranges in brackets